

Electroexcitation of the $\Delta(1232)_{\frac{3}{2}}^{+}$ and $\Delta(1600)_{\frac{3}{2}}^{+}$ in a light-front relativistic quark model

I. G. Aznauryan^{1,2} and V. D. Burkert¹¹Thomas Jefferson National Accelerator Facility, Newport News, Virginia 23606, USA²Yerevan Physics Institute, 375036 Yerevan, Armenia

(Received 11 June 2015; published 30 September 2015)

The magnetic-dipole form factor and the ratios R_{EM} and R_{SM} for the $\gamma^*N \rightarrow \Delta(1232)_{\frac{3}{2}}^{+}$ transition are predicted within the light-front relativistic quark model up to photon virtuality $Q^2 = 12 \text{ GeV}^2$. We also predict the helicity amplitudes of the $\gamma^*N \rightarrow \Delta(1600)_{\frac{3}{2}}^{+}$ transition assuming that the $\Delta(1600)_{\frac{3}{2}}^{+}$ is the first radial excitation of the ground state $\Delta(1232)_{\frac{3}{2}}^{+}$.

DOI: [10.1103/PhysRevC.92.035211](https://doi.org/10.1103/PhysRevC.92.035211)

PACS number(s): 12.39.Ki, 13.40.Gp, 13.40.Hq, 14.20.Gk

I. INTRODUCTION

One of the longstanding and intriguing problems of hadron physics is the identification of the states that can be assigned as the first radial excitations of the nucleon and $\Delta(1232)_{\frac{3}{2}}^{+}$. It is well recognized that the crucial role in the identification of the Roper resonance $N(1440)_{\frac{1}{2}}^{+}$ as a predominantly first radial excitation of the three-quark ($3q$) ground state belongs to the measurements by the CLAS Collaboration [1–6] that resulted in the determination of the electrocouplings of this resonance with the proton in a wide range of $Q^2 = 0.3\text{--}4.2 \text{ GeV}^2$. Comparison of the $\gamma^*p \rightarrow N(1440)_{\frac{1}{2}}^{+}$ transition amplitudes extracted from these data [7,8] with the predictions of the light-front relativistic quark models (LF RQM) [9,10] provided strong evidence for the $N(1440)_{\frac{1}{2}}^{+}$ as a member of the multiplet $[56,0^+]_r$, with additional non-three-quark contributions needed to describe the low- Q^2 behavior of the amplitudes.

Our goal in this paper is computation of the $\gamma^*N \rightarrow \Delta(1600)_{\frac{3}{2}}^{+}$ transition amplitudes in the LFRQM. Comparison of the results obtained in the quark model with the amplitudes that are expected to be extracted from experimental data will provide an important test for the commonly expected assignment of the $\Delta(1600)_{\frac{3}{2}}^{+}$ as the first radial excitation of the $\Delta(1232)_{\frac{3}{2}}^{+}$. Very recently, the CLAS data on the differential cross sections of the exclusive process $ep \rightarrow e\pi^+n$ were reported in the range of $Q^2 = 1.8\text{--}4 \text{ GeV}^2$ and the invariant mass range of the π^+n final state $W = 1.6\text{--}2.0 \text{ GeV}$ [11]. These data combined with the earlier CLAS data [6] on the cross sections and longitudinally polarized beam asymmetries for this reaction in the lower mass range $W = 1.15\text{--}1.69 \text{ GeV}$ and at close values of Q^2 allowed the extraction of the electroexcitation amplitudes of the resonances $N(1675)_{\frac{5}{2}}^{-}$, $N(1680)_{\frac{5}{2}}^{+}$, and $N(1710)_{\frac{1}{2}}^{+}$ in the third resonance region. The isotopic pairs of the resonances from this region, $\Delta(1600)_{\frac{3}{2}}^{+}$ and $N(1720)_{\frac{3}{2}}^{+}$, $\Delta(1620)_{\frac{1}{2}}^{-}$ and $N(1650)_{\frac{1}{2}}^{-}$, and $\Delta(1700)_{\frac{3}{2}}^{-}$ and $N(1700)_{\frac{3}{2}}^{-}$, could not be separated from each other using data from a single isospin channel. Currently new data are in preparation by the CLAS Collaboration for the $ep \rightarrow e\pi\pi^0$ process in the same kinematics region as the data in the $ep \rightarrow e\pi^+n$ channel [6,11], as well as at lower Q^2 . The two-channel analysis will allow the extraction of the

electroexcitation amplitudes of all resonances from the third resonance region including the $\Delta(1600)_{\frac{3}{2}}^{+}$.

The approach we use is based on the LF dynamics and is formulated in Refs. [12,13]. In numerous applications (see Refs. [10,14] and references therein), this approach was utilized for the investigation of nucleon form factors and electroexcitation of nucleon resonances.

In this work we study the electroexcitation of the $\Delta(1600)_{\frac{3}{2}}^{+}$ in parallel with that of the $\Delta(1232)_{\frac{3}{2}}^{+}$, where we complement the results obtained earlier in Ref. [14] by computing all three form factors that describe the transition $\gamma^*N \rightarrow \Delta(1232)_{\frac{3}{2}}^{+}$. In Refs. [15,16] it was shown that there are difficulties in the utilization of the LF approaches for hadrons with spin $J \geq 1$. In the approach of Ref. [13], these difficulties limit the number of transition amplitudes that can be investigated for the $\Delta(1232)_{\frac{3}{2}}^{+}$ and $\Delta(1600)_{\frac{3}{2}}^{+}$. Reliable results can be obtained only for two of the three transition form factors. They are based on the utilization of longitudinal components of the electromagnetic current $J_{em}^{0,z}$. For the $\Delta(1232)_{\frac{3}{2}}^{+}$, the results obtained for two transition form factors have been presented in Ref. [14]. In the present work, we complement these results by calculating the third transition form factor using $J_{em}^x + iJ_{em}^y$. As was shown in Ref. [13], these results are less reliable, as the matrix elements of transverse components of the electromagnetic current can contain contributions that violate impulse approximation, i.e., contributions of diagrams containing vertices such as $\gamma^* \rightarrow q\bar{q}$. Similar problem exists in the LF RQM of Refs. [9,16], where the requirement of rotational covariance cannot be satisfied without introducing two- and three-body current operators. For this reason, the results for the electroexcitation amplitudes for the resonances with spins $J = \frac{3}{2}$ are presented in Ref. [9] along with curves which show possible uncertainties that can be caused by the violation of the rotational covariance. When presenting our results we also demonstrate the uncertainties that can arise due to the inclusion of the transverse components of the electromagnetic current.

An important aspect in the comparison of the transition amplitudes obtained in theoretical approaches with the amplitudes extracted from experimental data is their sign (see, for example, Ref. [17]). The results on the $\gamma^*N \rightarrow N^*$ transition amplitudes extracted from experimental data contain

an additional sign related to the vertex of the resonance coupling to the final state hadrons. In the electroproduction of pions on nucleons this is the relative sign between the πNN^* and πNN vertices. For the Roper resonance, this sign was found in Refs. [9] and [10] using, respectively, the 3P_0 model and the approach based on partial conservation of axial current (PCAC) in the way suggested in Ref. [18]. The results obtained in both approaches are consistent with each other. In Sec. II, we determine the relative signs of the vertices πNN , $\pi N\Delta(1232)$, and $\pi N\Delta(1600)$ using the approach based on PCAC.

Our goals, and the ranges of Q^2 where we make predictions, for the resonances $\Delta(1232)_{\frac{3}{2}^+}$ and $\Delta(1600)_{\frac{3}{2}^+}$ are different. For the $\Delta(1600)_{\frac{3}{2}^+}$, we make predictions that are of interest to reveal the nature of this resonance using the existing and future CLAS data at $Q^2 < 4 \text{ GeV}^2$. For the $\Delta(1232)_{\frac{3}{2}^+}$, our goal is to make predictions up to 12 GeV^2 . These results will be important for the interpretation of future data on $\gamma^* p \rightarrow \Delta(1232)_{\frac{3}{2}^+}$ that are expected with the Jefferson Lab 12 GeV upgrade.

In Sec. II we present the LF RQM formalism to compute the $\gamma^* N \rightarrow \Delta$ transition amplitudes. The results for both resonances are presented and discussed in Sec. III and summarized in Sec. IV.

II. THE $\gamma^* N \rightarrow \Delta$ TRANSITION AMPLITUDES IN LF RQM

The $\gamma^* N \rightarrow \Delta(1232)_{\frac{3}{2}^+}$ and $\gamma^* N \rightarrow \Delta(1600)_{\frac{3}{2}^+}$ amplitudes have been evaluated within the approach of Ref. [13] where the LF RQM is formulated in the infinite momentum frame (IMF). The IMF is chosen in such a way that the initial hadron moves along the z axis with the momentum $P \rightarrow \infty$, the virtual photon momentum is $k^\mu = (\frac{M^2 - m^2 - Q_\perp^2}{4P}, \mathbf{Q}_\perp, -\frac{M^2 - m^2 - Q_\perp^2}{4P})$, the final hadron momentum is $P' = P + k$, and $Q^2 \equiv -k^2 = \mathbf{Q}_\perp^2$; m and M are masses of the nucleon and Δ , respectively. In this frame, the matrix elements of the electromagnetic current for the $\gamma^* N \rightarrow \Delta$ transition have the form

$$\begin{aligned} & \langle \Delta, S'_z | J_{em}^\mu | N, S_z \rangle |_{P \rightarrow \infty} \\ & = 3e Q_a \int \Psi'^+(p'_a, p'_b, p'_c) \Gamma_a^\mu \Psi(p_a, p_b, p_c) d\Gamma, \end{aligned} \quad (1)$$

where S_z and S'_z are the projections of the hadron spins on the z direction. In Eq. (1), it is supposed that the photon interacts with quark a (the quarks in hadrons are denoted by a, b, c); Q_a is the charge of this quark in units of e ($e^2/4\pi = 1/137$); Ψ and Ψ' are wave functions in the vertices $N(\Delta) \leftrightarrow 3q$; p_i and p'_i ($i = a, b, c$) are the quark momenta in IMF; $d\Gamma$ is the phase space volume; Γ_a^μ corresponds to the vertex of the quark interaction with the photon:

$$x_a \Gamma_a^x = 2p_{ax} + Q_x + i Q_y \sigma_z^{(a)}, \quad (2)$$

$$x_a \Gamma_a^y = 2p_{ay} + Q_y - i Q_x \sigma_z^{(a)}, \quad (3)$$

$$\Gamma_a^0 = \Gamma_a^z = 2P, \quad (4)$$

where x_a is the fraction of the initial hadron momentum carried by the quark.

Let \mathbf{q}_i ($i = a, b, c$) be the three-momenta of initial quarks in their center-of-mass system (c.m.s.): $\mathbf{q}_a + \mathbf{q}_b + \mathbf{q}_c = 0$. The sets of the quark three-momenta in the IMF and in the c.m.s. of the quarks are related as follows:

$$\mathbf{p}_i = x_i \mathbf{P} + \mathbf{q}_{i\perp}, \quad \sum_i x_i = 1. \quad (5)$$

According to results of Ref. [13], the wave function Ψ is related to the wave function in the c.m.s. of quarks through Melosh matrices [19]:

$$\Psi = U^+(p_a) U^+(p_b) U^+(p_c) \Psi_{fss} \Phi(\mathbf{q}_a, \mathbf{q}_b, \mathbf{q}_c). \quad (6)$$

Here we have separated the flavor-spin-space (Ψ_{fss}) and spatial (Φ) parts of the c.m.s. wave function. The Melosh matrices are

$$U(p_i) = \frac{m_q + M_0 x_i + i \epsilon_{lm} \sigma_l q_{im}}{\sqrt{(m_q + M_0 x_i)^2 + \mathbf{q}_{i\perp}^2}}, \quad (7)$$

where m_q is the quark mass and M_0 is the invariant mass of the system of initial quarks:

$$M_0^2 = \left(\sum_i p_i \right)^2 = \sum_i \frac{\mathbf{q}_{i\perp}^2 + m_q^2}{x_i}. \quad (8)$$

In the c.m.s. of quarks,

$$M_0 = \sum_i \omega_i, \quad \omega_i = \sqrt{m_q^2 + \mathbf{q}_i^2}, \quad q_{iz} + \omega_i = M_0 x_i. \quad (9)$$

For the final state quarks, the quantities defined by Eqs. (5)–(9) are expressed through p'_i , \mathbf{q}'_i , and M'_0 . The phase space volume in Eq. (1) has the form

$$d\Gamma = (2\pi)^{-6} \frac{d\mathbf{q}_{b\perp} d\mathbf{q}_{c\perp} dx_b dx_c}{4x_a x_b x_c}. \quad (10)$$

To study sensitivity to the form of the quark wave function, we employed two forms of the spatial wave function:

$$\Phi_{N(\Delta)}^{(1)} = N_{N(\Delta)}^{(1)} \exp(-M_0^2/6\alpha_1^2), \quad (11)$$

$$\Phi_{\Delta_r}^{(1)} = N_{\Delta_r}^{(1)} (\beta_1^2 - M_0^2) \exp(-M_0^2/6\alpha_1^2) \quad (12)$$

and

$$\Phi_{N(\Delta)}^{(2)} = N_{N(\Delta)}^{(2)} \exp[-(\mathbf{q}_a^2 + \mathbf{q}_b^2 + \mathbf{q}_c^2)/2\alpha_2^2], \quad (13)$$

$$\begin{aligned} \Phi_{\Delta_r}^{(2)} &= N_{\Delta_r}^{(2)} [\beta_2^2 - (\mathbf{q}_a^2 + \mathbf{q}_b^2 + \mathbf{q}_c^2)] \\ &\times \exp[-(\mathbf{q}_a^2 + \mathbf{q}_b^2 + \mathbf{q}_c^2)/2\alpha_2^2] \end{aligned} \quad (14)$$

that were used, respectively, in Refs. [12,13] and [9]. The parameters N and β are determined by the conditions

$$\int \Phi_{N(\Delta, \Delta_r)}^2 d\Gamma = 1, \quad \int \Phi_{N(\Delta)} \Phi_{\Delta_r} d\Gamma = 0. \quad (15)$$

To distinguish between ground state $\Delta(1232)$ and the $\Delta(1600)$, considered to be a member of the multiplet $[56, 0^+]_r$, we have used in Eqs. (11)–(15) notations Δ and Δ_r .

Other parameters of the model, namely, the quark mass m_q and the oscillator parameter α , were found in Ref. [14] from the description of nucleon form factors up to $Q^2 = 16 \text{ GeV}^2$. For the spatial wave functions (11) and (13), they have,

respectively, the following form:

$$\alpha_1 = 0.37 \text{ GeV}, \quad m_q^{(1)}(Q^2) = \frac{0.22 \text{ GeV}}{1 + Q^2/56 \text{ GeV}^2}, \quad (16)$$

$$\alpha_2 = 0.41 \text{ GeV}, \quad m_q^{(2)}(Q^2) = \frac{0.22 \text{ GeV}}{1 + Q^2/18 \text{ GeV}^2}. \quad (17)$$

For both resonances, the results for the transition amplitudes obtained with the wave functions (11,12) and (13,14) and corresponding parameters (16) and (17) turned out to be very close to each other.

Electroexcitation of the states with $J^P = \frac{3}{2}^{+}$ on the nucleon is described by three form factors $G_1(Q^2)$, $G_2(Q^2)$, and $G_3(Q^2)$, which we define according to Refs. [17,20] in the following way:

$$\langle \Delta, J^P = \frac{3}{2}^{+} | J_{em}^{\mu} | N \rangle \equiv e \bar{u}_v(P') \gamma_5 \Gamma^{\nu\mu} u(P), \quad (18)$$

$$\Gamma^{\nu\mu}(Q^2) = G_1 \mathcal{H}_1^{\nu\mu} + G_2 \mathcal{H}_2^{\nu\mu} + G_3 \mathcal{H}_3^{\nu\mu}, \quad (19)$$

$$\mathcal{H}_1^{\nu\mu} = \not{k} g^{\nu\mu} - k^{\nu} \gamma^{\mu}, \quad (20)$$

$$\mathcal{H}_2^{\nu\mu} = k^{\nu} P'^{\mu} - (k P') g^{\nu\mu}, \quad (21)$$

$$\mathcal{H}_3^{\nu\mu} = k^{\nu} k^{\mu} - k^2 g^{\nu\mu}, \quad (22)$$

where $u(P)$ and $u_v(P')$ are, respectively, the Dirac and Rarita-Schwinger spinors. These form factors have been found through the matrix elements (1) using the relations

$$\begin{aligned} & \frac{1}{2P} \left\langle \Delta, \frac{3}{2} \left| J_{em}^{0,z} \right| N, \frac{1}{2} \right\rangle \Big|_{P \rightarrow \infty} \\ &= -\frac{Q}{\sqrt{2}} \left[G_1(Q^2) + \frac{M-m}{2} G_2(Q^2) \right], \end{aligned} \quad (23)$$

$$\frac{1}{2P} \left\langle \Delta, \frac{3}{2} \left| J_{em}^{0,z} \right| N, -\frac{1}{2} \right\rangle \Big|_{P \rightarrow \infty} = \frac{Q^2}{2\sqrt{2}} G_2(Q^2), \quad (24)$$

$$\left\langle \Delta, \frac{3}{2} \left| J_{em}^x + i J_{em}^y \right| N, -\frac{1}{2} \right\rangle \Big|_{P \rightarrow \infty} = \frac{Q^3}{\sqrt{2}} G_3(Q^2). \quad (25)$$

The relations between form factors $G_1(Q^2)$, $G_2(Q^2)$, and $G_3(Q^2)$ and the $\gamma^* N \rightarrow \Delta(\frac{3}{2}^{+})$ helicity amplitudes and the Jones-Scadron form factors $G_M(Q^2)$, $G_E(Q^2)$, and $G_C(Q^2)$ [21] are given in the Appendix.

In the approach based on PCAC, the relative signs of the πNN , $\pi N \Delta(1232)$, and $\pi N \Delta(1600)$ vertices are determined according to Refs. [10,15] by the relative signs of the expressions

$$I_{NA} \equiv \int \frac{(m_q + M_0 x_a)^2 - \mathbf{q}_{a\perp}^2}{(m_q + M_0 x_a)^2 + \mathbf{q}_{a\perp}^2} \Phi_N(M_0^2) \Phi_A(M_0^2) d\Gamma, \quad (26)$$

where A denotes the states N , $\Delta(1232)$, and $\Delta(1600)$. Numerical calculation of I_{NN} , $I_{N\Delta(1232)}$, and $I_{N\Delta(1600)}$ with the wave functions (11)–(14) gives positive relative signs for the πNN , $\pi N \Delta(1232)$, and $\pi N \Delta(1600)$ vertices.

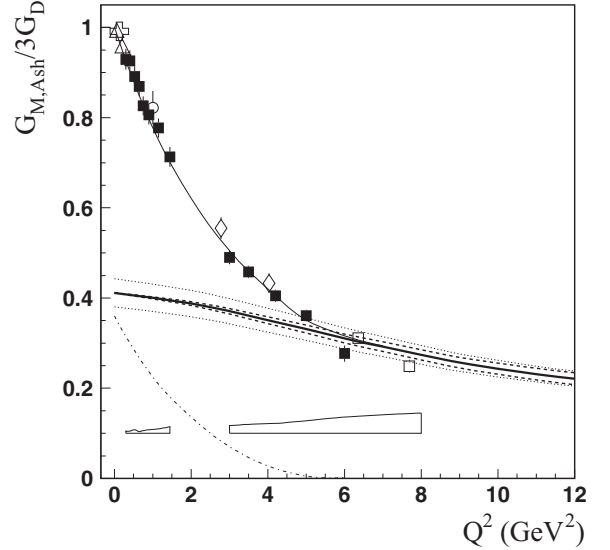


FIG. 1. The form factor $G_{M,Ash}(Q^2)$ for the $\gamma^* p \rightarrow \Delta(1232)_{\frac{3}{2}}^{+}$ transition relative to $3G_D$: $G_D(Q^2) = 1/(1 + \frac{Q^2}{0.71 \text{ GeV}^2})$. The full boxes are the CLAS data extracted in the analysis of Ref. [8]; the open boxes correspond to the data from Ref. [23]. The bands show the model uncertainties of these data [8,17]. The thin solid curve is the result of the global analysis of the Mainz group [24]. The results from other experiments are open triangles [25–27], open cross [28–30], open rhombuses [31], and open circle [32,33]. The thick solid curve presents our results. The dashed curves demonstrate the sensitivity of these results to the form factor $G_3(Q^2)$ (25); they correspond to $G_3(Q^2)$ taken with $\pm 50\%$ deviation from the values obtained using the relation (25). The dotted curves show the uncertainty of our results (given by the solid curve) that is caused by the uncertainty of c_Δ (31). The dashed-dotted curve is the meson-baryon contribution from Refs. [34,35].

III. RESULTS

A. The $\Delta(1232)_{\frac{3}{2}}^{+}$ resonance

We present the results for the $\Delta(1232)_{\frac{3}{2}}^{+}$ in terms of the $\gamma^* p \rightarrow \Delta(1232)_{\frac{3}{2}}^{+}$ magnetic-dipole transition form factor in the Ash convention [22] (Fig. 1) and the ratios $R_{EM} \equiv \text{Im } E_{1+}^{3/2} / \text{Im } M_{1+}^{3/2}$ and $R_{SM} \equiv \text{Im } S_{1+}^{3/2} / \text{Im } M_{1+}^{3/2}$ (Fig. 2). These observables are commonly used to present the results on the $\Delta(1232)_{\frac{3}{2}}^{+}$ extracted from experimental data on the electroproduction of pions on nucleons. The $\gamma^* p \rightarrow \Delta(1232)_{\frac{3}{2}}^{+}$ magnetic-dipole form factor in the Ash convention is related to the Jones-Scadron form factor defined in the Appendix as follows:

$$G_{M,Ash}(Q^2) = \frac{G_M(Q^2)}{\sqrt{1 + \frac{Q^2}{(M+m)^2}}}. \quad (27)$$

The ratios R_{EM} and R_{SM} are related to the Jones-Scadron form factors by

$$R_{EM} = -\frac{G_E}{G_M}, \quad R_{SM} = -\frac{G_C}{G_M} \frac{K}{2m}, \quad (28)$$

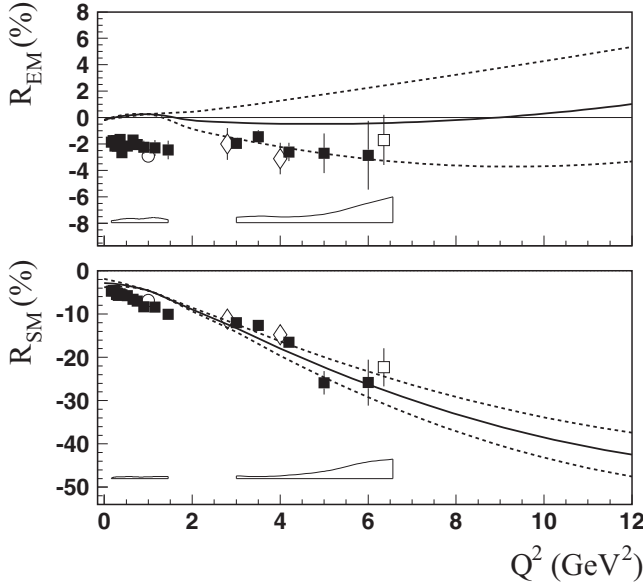


FIG. 2. The ratios R_{EM} and R_{SM} for the $\gamma^*p \rightarrow \Delta(1232)_{\frac{3}{2}}^+$ transition. The legend for experimental data and thick solid and dashed curves is as for Fig. 1.

where K is the virtual photon three-momentum in the c.m.s. of the reaction $\gamma^*N \rightarrow \pi N$:

$$K \equiv \frac{\sqrt{Q_+ Q_-}}{2M}, \quad Q_{\pm} \equiv (M \pm m)^2 + Q^2. \quad (29)$$

As mentioned in the Introduction, in the approach that we utilize [13], the results that are reliable are obtained through longitudinal components of the electromagnetic current $J_{em}^{0,z}$, i.e., the results for the form factors $G_1(Q^2)$ and $G_2(Q^2)$ [(23) and (24)]. These results have been presented and discussed in Ref. [14]. In this paper, we complement the results for $G_1(Q^2)$ and $G_2(Q^2)$ by calculating the third transition form factor $G_3(Q^2)$ using $J_{em}^x + iJ_{em}^y$ (25). This allows us to present the predictions in a more convenient way in terms of $G_{M, Ash}$ and R_{EM} and R_{SM} . In order to demonstrate the sensitivity of $G_{M, Ash}$, R_{EM} , and R_{SM} to the inclusion of the transverse components of the electromagnetic current, we also present in Figs. 1 and 2 results that correspond to the values of $G_3(Q^2)$ taken with $\pm 50\%$ deviation from the values obtained using the relation (25).

It is known that, at relatively small Q^2 , nearly massless pions generate pion-loop contributions that significantly alter the three-quark contribution to $\gamma^*p \rightarrow \Delta(1232)_{\frac{3}{2}}^+$. It is expected that the corresponding hadronic component, including contributions from other mesons, will be rapidly losing strength with increasing Q^2 . From the description of the data on pion electroproduction on protons within the dynamical reaction model [34,35], it follows that the contribution associated with the meson-baryon contribution to $\gamma^*p \rightarrow \Delta(1232)_{\frac{3}{2}}^+$ (dashed-dotted curve in Fig. 1) can be neglected above $Q^2 = 4 \text{ GeV}^2$. Therefore, the weight of the $3q$ contribution to the $\Delta(1232)_{\frac{3}{2}}^+$,

$$|\Delta(1232)| = c_{\Delta}|3q| + \dots, \quad (30)$$

was found in Ref. [14] from the description of the form factors $G_1(Q^2)$ and $G_2(Q^2)$ at $Q^2 > 4 \text{ GeV}^2$:

$$c_{\Delta} = 0.53 \pm 0.04. \quad (31)$$

The uncertainty of c_{Δ} is caused mainly by the systematic uncertainties of the data on $G_{M, Ash}(Q^2)$ at these Q^2 . We have used the value of c_{Δ} from Eq. (31) to find the three-quark contributions to $G_{M, Ash}(Q^2)$ and R_{EM} and R_{SM} , which are presented in Figs. 1 and 2.

From the discussion above, it follows that, at $Q^2 < 4 \text{ GeV}^2$, meson-baryon contributions alter the three-quark contribution to $\gamma^*p \rightarrow \Delta(1232)_{\frac{3}{2}}^+$. With this, for the magnetic-dipole form factor, these contributions definitely result in better agreement with experiment [34–38]. Above 4–5 GeV^2 , we expect that the $\gamma^*p \rightarrow \Delta(1232)_{\frac{3}{2}}^+$ transition will be determined by the three-quark contribution only. Therefore, we consider our results at these Q^2 as predictions for the $\gamma^*p \rightarrow \Delta(1232)_{\frac{3}{2}}^+$ transition amplitudes obtained within the nonperturbative approach.

For the form factor $G_{M, Ash}(Q^2)$, the sensitivity of our predictions to the possible uncertainties of the form factor $G_3(Q^2)$ seems insignificant. According to our results, we expect that above 5 GeV^2 the behavior of the ratio $G_{M, Ash}(Q^2)/G_D(Q^2)$ will become more flat in comparison with that at lower Q^2 . A similar Q^2 dependence is observed for the proton magnetic form factor [39]. For the Jones-Scadron magnetic-dipole form factor $G_M(Q^2)$ and the proton magnetic form factor $G_{M,p}(Q^2)$, the Q^2 dependences at $Q^2 = 5\text{--}12 \text{ GeV}^2$ practically coincide.

For the ratios R_{EM} and R_{SM} , the sensitivity of predictions to $G_3(Q^2)$ is more significant. Nevertheless, for the ratio R_{SM} one can conclude that it will continue to grow and within the $Q^2 = 12 \text{ GeV}^2$ limit will not reach the value predicted in pQCD, i.e., $R_{SM} \rightarrow \text{const}$ with undefined sign and magnitude. On the other hand, in holographic QCD in the large- N_c limit the R_{SM} ratio is predicted at the specific asymptotic value $R_{SM} \rightarrow -100\%$ [40]. The data show the correct trend, but are projected to reach only 40% to 50% of that value at $Q^2 \leq 12 \text{ GeV}^2$.

B. The $\Delta(1600)_{\frac{3}{2}}^+$ resonance

The results for the resonance $\Delta(1600)_{\frac{3}{2}}^+$, considered to be the first radial excitation of the ground state $\Delta(1232)_{\frac{3}{2}}^+$, are presented in Fig. 3 in terms of the $\gamma^*p \rightarrow \Delta(1600)_{\frac{3}{2}}^+$ helicity amplitudes. The predictions of the LFRQM approach from Ref. [9] are also shown. The common sign of the amplitudes has been found in our approach and in Ref. [9] due to additional computation of the relative signs of the πNN , $\pi N\Delta(1232)$, and $\pi N\Delta(1600)$ vertices using different approaches. Both approaches predict specific behavior of the transverse amplitudes: being large and negative at $Q^2 = 0$, they change signs at $Q^2 = 0.2\text{--}0.3 \text{ GeV}^2$ and become quite large and positive.

We want to emphasize that our predictions are related to the $|3q\rangle$ content of the $\Delta(1600)_{\frac{3}{2}}^+$. In a relation similar to Eq. (30) for this resonance, the coefficient c_{Δ_r} , as well the meson-baryon contributions are unknown, and only an analysis of the experimental transition amplitudes can determine

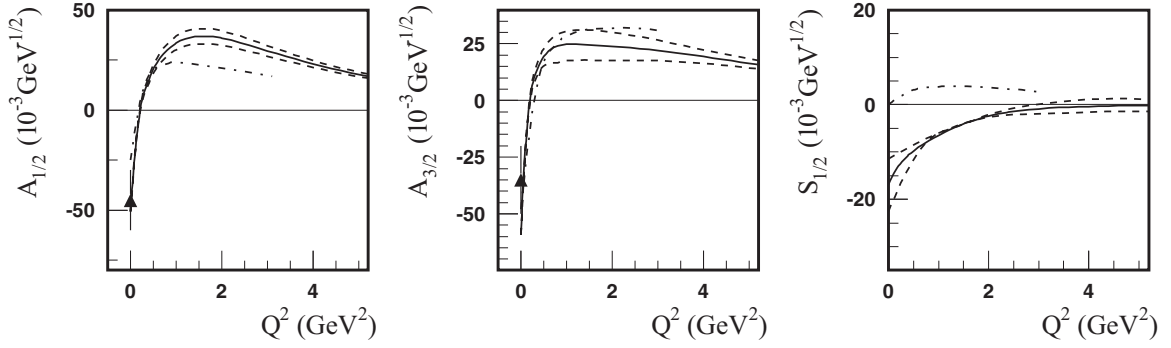


FIG. 3. Helicity amplitudes for the $\gamma^* p \rightarrow \Delta(1600)_{\frac{3}{2}}^{3+}$ transition. The full triangles at $Q^2 = 0$ are the Review of Particle Physics (RPP) estimates [41]. The thick solid curve presents our LF RQM predictions. The legend for dashed curves is as for Fig. 1. The dashed-dotted curves present the predictions from Ref. [9].

the relative strength of the three-quark and meson-baryon contributions. We remark that a similar situation occurred with the transition $\gamma^* p \rightarrow N(1440)_{\frac{1}{2}}^{1+}$, where the LF RQM approaches [9,10] predicted a very rapid sign change of the transverse amplitude near $Q^2 = 0.2$ GeV² to large positive value with a relatively slow fall-off above $Q^2 > 1.5$ GeV². The data showed a larger amplitude at the photon point and a significant shift of the zero-crossing to higher Q^2 , which could be attributed to meson-baryon contributions. The sign change of this amplitude and its high Q^2 behavior allowed then the identification of the $|3q\rangle$ content of the state as a radial excitation of the proton [7,8]. For the $\Delta(1600)_{\frac{3}{2}}^{3+}$ we may expect a similar situation.

We mention that the LF RQM predictions for transverse amplitudes at $Q^2 = 0$ are in good agreement with experimental data. However, the coefficient c_{Δ} , is unknown yet. Therefore, we may not conclude that meson-baryon contributions are small. A crucial test will be the behavior at low Q^2 , namely the position of the zero-crossing, and also the behavior at $Q^2 = 2-4$ GeV², where we expect that the meson-baryon contributions can be neglected. Experimental data at $Q^2 = 2-4$ GeV² will allow us to find the coefficient c_{Δ} . Then the real comparison of the quark model predictions for the $\gamma^* p \rightarrow \Delta(1600)_{\frac{3}{2}}^{3+}$ amplitudes with experimental data can be made with subsequent conclusions on the meson-baryon contributions.

IV. SUMMARY

We have employed the LF RQM to evaluate the quark core contribution to the transition $\gamma^* N \rightarrow \Delta(1232)_{\frac{3}{2}}^{3+}$ and to predict the $\gamma^* N \rightarrow \Delta(1600)_{\frac{3}{2}}^{3+}$ helicity amplitudes assuming that the $\Delta(1600)_{\frac{3}{2}}^{3+}$ is the first radial excitation of the ground state $\Delta(1232)_{\frac{3}{2}}^{3+}$. Our previous evaluation of the three-quark core contribution to the $\Delta(1232)_{\frac{3}{2}}^{3+}$ based on the $\gamma^* N \rightarrow \Delta(1232)_{\frac{3}{2}}^{3+}$ data up to $Q^2 = 7.5$ GeV² allowed us to make projections into unmeasured territory of $Q^2 \leq 12$ GeV². This region may be covered in upcoming measurements with CLAS12 at the Jefferson Lab 12 GeV upgrade. The projections are made for the magnetic-dipole form factor and electric and scalar quadrupole ratios $R_{EM}(Q^2)$ and $R_{SM}(Q^2)$. For

the $\Delta(1600)_{\frac{3}{2}}^{3+}$, the predictions are made in the range $Q^2 \leq 5$ GeV². The predicted very rapid transition from large negative values at the real photon point to large positive values with maxima near $Q^2 = 1-2$ GeV² for the two transverse amplitudes should be readily accessible to experimental exploration.

ACKNOWLEDGMENTS

This work was supported by the U.S. Department of Energy, Office of Science, Office of Nuclear Physics, under Contract No. DE-AC05-06OR23177, and the National Science Foundation, State Committee of Science of the Republic of Armenia, Grant No. 15T-1C223.

APPENDIX A: THE RELATIONS BETWEEN THE $\gamma^* N \rightarrow \Delta(\frac{3}{2}^+)$ FORM FACTORS AND HELICITY AMPLITUDES

The relations between the form factors $G_1(Q^2)$, $G_2(Q^2)$, and $G_3(Q^2)$ defined by Eqs. (18)–(22) and the $\gamma^* N \rightarrow \Delta(\frac{3}{2}^+)$ helicity amplitudes are [17,20]

$$A_{1/2} = h_3 X, \quad A_{3/2} = \sqrt{3} h_2 X, \quad S_{1/2} = h_1 \frac{K}{\sqrt{2M}} X, \quad (\text{A1})$$

where

$$h_1(Q^2) = 4M G_1(Q^2) + 4M^2 G_2(Q^2) + 2(M^2 - m^2 - Q^2) G_3(Q^2), \quad (\text{A2})$$

$$h_2(Q^2) = -2(M + m) G_1(Q^2) - (M^2 - m^2 - Q^2) G_2(Q^2) + 2Q^2 G_3(Q^2), \quad (\text{A3})$$

$$h_3(Q^2) = -\frac{2}{M} [Q^2 + m(M + m)] G_1(Q^2) + (M^2 - m^2 - Q^2) G_2(Q^2) - 2Q^2 G_3(Q^2), \quad (\text{A4})$$

$$X \equiv e \sqrt{\frac{Q_-}{48m(M^2 - m^2)}}. \quad (\text{A5})$$

The Jones-Scadron form factors $G_M(Q^2)$, $G_E(Q^2)$, and $G_C(Q^2)$ [21] are defined by

$$G_M(Q^2) = -Y(\sqrt{3}A_{3/2} + A_{1/2}), \quad (\text{A6})$$

$$G_E(Q^2) = -Y(A_{3/2}/\sqrt{3} - A_{1/2}), \quad (\text{A7})$$

$$G_C(Q^2) = 2\sqrt{2}\frac{M}{K}YS_{1/2}, \quad (\text{A8})$$

$$Y \equiv \frac{m}{e(M+m)}\sqrt{\frac{2m(M^2 - m^2)}{Q_-}}. \quad (\text{A9})$$

-
- [1] K. Joo *et al.* (CLAS Collaboration), *Phys. Rev. Lett.* **88**, 122001 (2002).
- [2] K. Joo *et al.* (CLAS Collaboration), *Phys. Rev. C* **68**, 032201 (2003).
- [3] K. Joo *et al.* (CLAS Collaboration), *Phys. Rev. C* **70**, 042201 (2004).
- [4] H. Egayan *et al.* (CLAS Collaboration), *Phys. Rev. C* **73**, 025204 (2006).
- [5] A. Biselli *et al.* (CLAS Collaboration), *Phys. Rev. C* **78**, 045204 (2008).
- [6] K. Park *et al.* (CLAS Collaboration), *Phys. Rev. C* **77**, 015208 (2008).
- [7] I. G. Aznauryan *et al.* (CLAS Collaboration), *Phys. Rev. C* **78**, 045209 (2008).
- [8] I. G. Aznauryan *et al.* (CLAS Collaboration), *Phys. Rev. C* **80**, 055203 (2009).
- [9] S. Capstick and B. D. Keister, *Phys. Rev. D* **51**, 3598 (1995).
- [10] I. G. Aznauryan, *Phys. Rev. C* **76**, 025212 (2007).
- [11] K. Park *et al.* (CLAS Collaboration), *Phys. Rev. C* **91**, 045203 (2015).
- [12] L. A. Kondratyuk and M. V. Terentev, *Yad. Fiz.* **31**, 1087 (1980).
- [13] I. G. Aznauryan, A. S. Bagdasaryan, and N. L. Ter-Isaakyan, *Phys. Lett. B* **112**, 393 (1982); *Yad. Fiz.* **36**, 1278 (1982).
- [14] I. G. Aznauryan and V. D. Burkert, *Phys. Rev. C* **85**, 055202 (2012).
- [15] I. G. Aznauryan and A. S. Bagdasaryan, *Sov. J. Nucl. Phys.* **41**, 158 (1985).
- [16] B. D. Keister, *Phys. Rev. D* **49**, 1500 (1994).
- [17] I. G. Aznauryan and V. D. Burkert, *Prog. Part. Nucl. Phys.* **67**, 1 (2012).
- [18] F. J. Gilman, M. Kugler, and S. Meshkov, *Phys. Rev. D* **9**, 715 (1974).
- [19] H. J. Melosh, *Phys. Rev. D* **9**, 1095 (1974).
- [20] R. C. E. Devenish, T. S. Eizenschitz, and J. G. Körner, *Phys. Rev. D* **14**, 3063 (1976).
- [21] H. F. Jones and M. D. Scadron, *Ann. Phys. (NY)* **81**, 1 (1973).
- [22] W. W. Ash, *Phys. Lett. B* **24**, 165 (1967).
- [23] A. N. Villano *et al.*, *Phys. Rev. C* **80**, 035203 (2009).
- [24] D. Drechsel, S. Kamalov, and L. Tiator, *Eur. Phys. J. A* **34**, 69 (2007).
- [25] S. Stave *et al.*, *Eur. Phys. J. A* **30**, 471 (2006).
- [26] N. F. Sparveris *et al.*, *Phys. Lett. B* **651**, 102 (2007).
- [27] S. Stave *et al.*, *Phys. Rev. C* **78**, 025209 (2008).
- [28] C. Mertz *et al.*, *Phys. Rev. Lett.* **86**, 2963 (2001).
- [29] C. Kunz *et al.*, *Phys. Lett. B* **564**, 21 (2003).
- [30] N. F. Sparveris *et al.*, *Phys. Rev. Lett.* **94**, 022003 (2005).
- [31] V. V. Frolov *et al.*, *Phys. Rev. Lett.* **82**, 45 (1999).
- [32] J. J. Kelly *et al.*, *Phys. Rev. Lett.* **95**, 102001 (2005).
- [33] J. J. Kelly *et al.*, *Phys. Rev. C* **75**, 025201 (2007).
- [34] T. Sato and T.-S. H. Lee, *Phys. Rev. C* **63**, 055201 (2001).
- [35] V. D. Burkert and T.-S. H. Lee, *Int. J. Mod. Phys. E* **13**, 1035 (2004).
- [36] K. Bermuth, D. Drechsel, L. Tiator, and J. B. Seaborn, *Phys. Rev. D* **37**, 89 (1988).
- [37] D. H. Lu, A. W. Thomas, and A. G. Williams, *Phys. Rev. C* **55**, 3108 (1997).
- [38] A. Faessler, T. Gutsche, B. R. Holstein, V. E. Lyubovitskij, D. Nicmorus, and K. Pumsa-ard, *Phys. Rev. D* **74**, 074010 (2006).
- [39] M. K. Jones *et al.*, *Phys. Rev. Lett.* **84**, 1398 (2000).
- [40] H. R. Grigoryan, T.-S. H. Lee, and H. U. Yee, *Phys. Rev. D* **80**, 055006 (2009).
- [41] K. A. Olive *et al.* (Particle Data Group Collaboration), *Chin. Phys. C* **38**, 090001 (2014).